JMEPEG (2006) 15:370-375
DOI: 10.1361/105994906X113697

1059-9495/$19.00

Surface Modification of Rutile TiO_2 by Submerged Arc Discharge for Improved Photoreactivity

Y. Ma, S. Manolache, F. Denes, J. Cho, and R. Timmons

(Submitted December 9, 2005; in revised form April 24, 2006)

Titanium dioxide is well known for its photocatalytic activity, but it works effectively only in the ultraviolet (UV) range. Given the relatively low flux of solar UV that reaches earth, the potential of exploring its photocatalytic capacity for environmental protection applications is very limited. In this study, rutile, the least photocatalytic of the three existing titanium dioxide crystalline forms, was suspended in water or acetonitrile and treated with oxygen or argon plasmas, using a novel dense-medium plasma technology (submerged arc discharge). As a result of the plasma treatment, rutile particles were doped with various trace elements that originated in electrodes made of different metals. Subsequent analyses show that the photocatalytic capacity of plasma-modified rutile is comparable to or even better than that of unmodified anatase, the most photocatalytic form of titanium dioxides. The color change of TiO_2 samples after plasma treatment indicates that the modified rutile absorbs visible light and may therefore work as a photocatalyst in the visible range. Given the fact that rutile can be produced in large quantity more easily and cheaply than can anatase, these results are very encouraging and open up possibilities in using rutile for photocatalytic applications in the visible range.

Keywords: dense-medium plasma, iron, photocatalysis, plasma, rutile, titania

1. Introduction

In recent years, titanium dioxide has been at the center of an intensive international effort of the study of its photocatalytic properties as an efficient way for chemical utilization of solar energy. When irradiated with light, TiO_2 generates electrons and holes; these give it strong reducing and oxidizing powers, respectively, as illustrated in Fig. 1. Generally speaking, attention has been focused on its oxidizing power. When brought into contact with the surface of TiO_2, most organic micropollutants, including dioxins in emission gas, can be ultimately decomposed into carbon dioxide and water by the effect of the holes with their highly oxidative potential. With its strong photocatalytic capacity, TiO_2 can be used in many pollution-control applications, such as deodorization, antibacterial properties, emission gas treatment, self-cleaning, anti-staining properties, water treatment, and water splitting (Ref 1, 2).

However, unmodified TiO_2 is not an efficient photocatalyst. Among the three existing polymorphs of TiO_2, anatase and rutile have been widely studied. It has been generally accepted that anatase is more photocatalytic than rutile because of differences in their band gap structures. One problem in using anatase as a photocatalyst is its large band gap, which is 3.2 eV and leads to a photoresponse wavelength <387 nm (in the UV light region). As solar energy contains only ~5% of UV light, unmodified anatase is not a very efficient photocatalyst (Ref 3). Similar problems exist with rutile, although its absorption wavelength is closer to that of violet light at 413 nm. Therefore, to exploit the inherent photocatalytic capacity of TiO_2, it is desirable to use modified TiO_2 in order to improve its effectiveness.

Another reason it is important to modify TiO_2 is that, as a

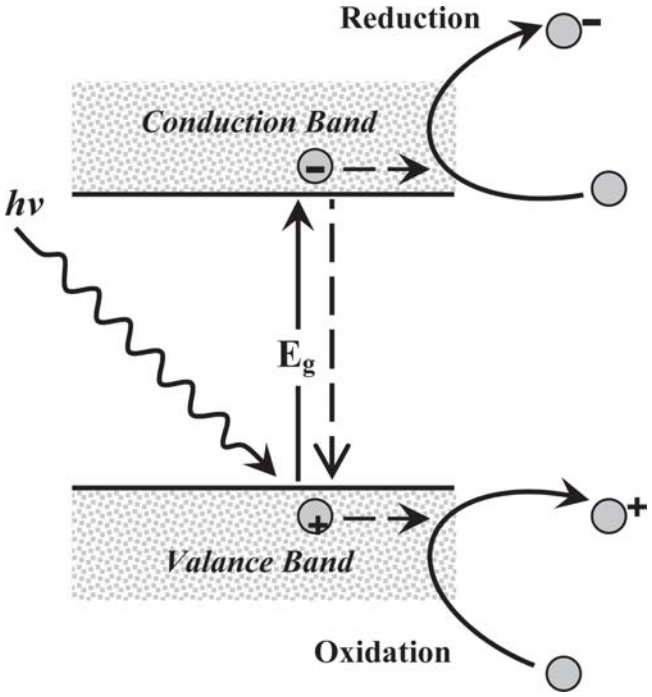

Fig. 1 Mechanism of photocatalysis, showing the photoexcitation process, formation of electron/hole pairs, and reduction/oxidation reactions that occur at the surface of photocatalyst

This paper was presented at the Third International Surface Engineering Congress and Exposition held August 2-4, 2004 in Orlando, FL.

Y. Ma, S. Manolache, and **F. Denes,** Center for Plasma-Aided Manufacturing, University of Wisconsin, Madison, WI 53706; **J. Cho** and **R. Timmons,** Department of Chemistry & Biochemistry, University of Texas, Arlington, TX 76019. Contact e-mail: denes@engr.wisc.edu.

photocatalyst, it is most often used as a powder suspended in a liquid medium. Handling of such powders and their subsequent removal can be fairly difficult and expensive processes. Therefore, recent research has focused on using TiO_2 in its immobilized form, e.g., as thin films on supports. However, due to the more limited surface areas, a smaller quantity of available catalysts, and increased vulnerability to contamination by impurities, the immobilized titania exhibits low photocatalytic efficiency and must be modified to have any meaningful impact.

Many studies have been dedicated to modification of TiO_2 to improve its photocatalytic properties. It seems that, recently, most studies have focused their efforts on doping TiO_2 with noble metals (e.g., Ag, Pt, and Au) (Ref 4-6) or transition metals (e.g., Ni, Fe) (Ref 7, 8). Traditional procedures to prepare these metal-coated or metal-doped TiO_2 materials include chemical, electrochemical, and photodeposition methods, such as precipitation deposition, incipient wet-impregnation, sol-gel methods, or photoreduction under UV irradiation. The idea behind these methods is to form electron-trapping sites within the TiO_2 substrate or close to its surface, thus reducing the undesirable recombination of holes and electrons and thereby liberating holes to participate in photon-induced reactions. However, the detailed influence of metal doping on the photoelectrochemical behavior is not yet fully understood (Ref 9). Nitrogen- and sulfur-doped TiO_2 were also investigated (Ref 10, 11), although the latter suffers from degradation of photocatalytic activity caused by possible catalytic poisoning. Recently, several studies reported have reported using carbon as a doping material to replace the lattice oxygen atoms in both rutile and anatase (Ref 12-15). Carbon-doped TiO_2 has shown significant improvement in photocatalysis. In one of these studies, the authors claimed that the carbon-doped rutile layer is five times more active than nitrogen-doped TiO_2 in the degradation of 4-chlorophenol by artificial light (Ref 13).

In this study, rutile, the least photocatalytic crystalline form of TiO_2, was selected for modification to improve its photocatalytic capacity. The more catalytic anatase was also treated in this study, but it was not emphasized. In fact, studies from other researchers have shown that the generally accepted notion that anatase is more photoactive than rutile may not be true for all conditions or reactions (Ref 16). The commonly used P25 TiO_2 consists of a large fraction of anatase, but it has been demonstrated that many of the anatase particles are covered by a thin layer of rutile, which means some of the anatase studies have actually been conducted on rutile surfaces (Ref 17). In addition, compared with rutile, it is more difficult and expensive to produce anatase in large quantities. In light of these considerations, the authors believe it is more important that they focus their efforts on improving the photocatalytic ability of rutile.

A description of the patented dense-medium plasma (DMP) technology is presented herein. DMP allows initiation and sustained discharges in a coexisting liquid/vapor medium at atmospheric pressure. It offers a significantly higher efficiency for the processing of liquid-phase materials in comparison to other existing plasma technologies. In this study, rutile was suspended in either distilled water or acetonitrile and then treated using the DMP reactor with various electrodes (i.e., doping materials), different plasma gases, and different treatment times. In addition, in suspensions of rutile in acetonitrile, carbon nanoparticles were deposited onto the surfaces of rutile particles. The photocatalytic capacity of modified rutile was evaluated and compared with that of anatase.

2. Materials and Methods

2.1 Materials and Characterization Techniques

Rutile (>99.9%, <5 μm) and acetonitrile (99%) were purchased from Aldrich Co. (St. Louis, MO). Anatase (P25) is from Degussa (Ridgefield Park, NJ). Argon was purchased from Liquid Carbonic Specialty Gas Corp. (San Carlos, CA) and was used as cavitation-generating inert gas during the synthesis and as plasma gas during the surface functionalizations.

Scanning electron microscope (SEM) images were collected using a LEO 1530 field emission SEM (LEO Electron Microscopy, Inc., Thornwood, NY). Samples were mounted using a piece of double-sided copper tape and were coated with gold by sputter deposition. The sputtering device was a Denton Vacuum Inc. (Moorestown, NJ) Desk II system; sputtering gas (argon) pressure was 50 mtorr, sputtering current was 45 mA, and sputtering time was 10 s.

An Ultima ICP-AES inductively coupled plasma mass spectrometry (ICP-MS) instrument was used (Jobin-Yvon, Edison, NJ). The samples were wet-ashed and extracted with nitric acid and hydrogen peroxide at 140 °C and 100 psi for 25 min. They were then filtered into volumetric flasks, and elemental analyses were carried out.

A JASCO V-530 UV/vis spectrophotometer was used for measuring absorption of the dichromate solution (Jasco, Tokyo, Japan).

2.2 Plasma Treatment of Rutile

The DMP used in this study was designed and developed at the Center for Plasma-Aided Manufacturing, University of Wisconsin-Madison (Ref 18, 19). The DMP reactor provides initiation and sustained discharges at atmospheric pressure in a coexisting liquid/vapor medium and offers a significantly higher efficiency for the processing of liquid-phase materials or suspensions in comparison to existent plasma technologies.

Figure 2 shows the design of this DMP reactor. It is composed of a vacuum-tight cylindrical glass chamber wherein the liquid medium to be treated is contained. A set of electrodes is immersed within the liquid medium. The upper electrode has a ceramic disc cap, on top of which is located an array of metal pins. The lower electrode is basically a metal disc with three holes for the purpose of facilitating liquid circulation. Both electrodes can be made from selected metals, as dictated by the particular treatment. Distance between the electrodes can be adjusted as desired.

For plasma treatment, the upper electrode can be rotated at high speed (up to 5,000 rpm) whereas the lower electrode is stationary. Inert or reactive plasma gas is bubbled through the liquid medium from the bottom of the glass chamber. Combination of these two motions generates numerous microcavities between the electrodes. At this time, the direct current (dc) power supply is turned on and plasma is initiated within the microcavities. Active species (e.g., free radicals) diffuse toward the interface and react with the liquid medium. Rotation of the electrode also helps homogenize the microdischarges, activate a larger effective volume of fluid, pump fresh liquid medium into the discharge zone, and decrease the boundary

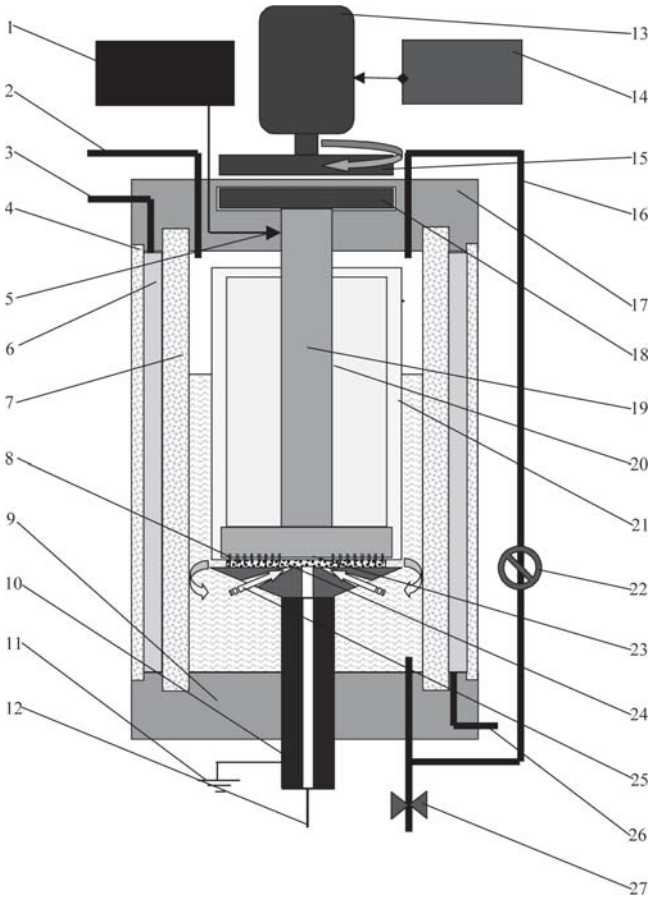

Fig. 2 Redesigned DMP reactor: (1) DC power supply; (2) gas evacuation point; (3, 26) coolant exit and inlet; (4, 7) glass cylinders; (5) electrical contact; (6) coolant; (8) ceramic-pin array; (9, 17) caps; (10) non-rotating electrode; (11) ground; (12) gas inlet; (13) motor; (14) digital controller; (15, 18) magnetic coupling system; (16) liquid inlet; (19) rotating electrode; (20) sealed volume; (21) quartz isolator; (22) recirculating pump; (23) pins; (24) electrical discharges; (25) recirculated flux; (27) valve

layers between the emission tips and the bulk liquid. A more detailed description of the DMP reactor can be found in our previous publications (Ref 18-20).

During a typical experiment, 4 g of TiO_2 is suspended in 200 mL of distilled water or acetonitrile. The suspension is well mixed by a magnetic stirrer and introduced into the glass chamber of the DMP reactor. Plasma gas is injected through the hollow, lower electrode at a flow rate of 2 sccm. Cooling of the reaction medium is started by a flow of tap water through the cooling jacket, and the rotation of the upper electrode is started at the desired angular speed. The discharge is initiated, and the plasma state is sustained for the preselected treatment time. After plasma treatment, the suspension is then filtered and washed several times. The resulting TiO_2 powders are dried in a vacuum oven at 50 °C for at least 12 h before being ground and sealed for subsequent analyses to evaluate their photocatalytic capacity. The following experimental conditions were used during the actual plasma treatment: type of electrodes, Fe or Ag or Ti; DC voltage, 200 V; current, 1 A; angular speed of the rotating electrode, 1000 rpm; plasma gas, Ar or O_2; temperature of the reaction media, 18 °C; treatment time, 1, 2, or 3 min.

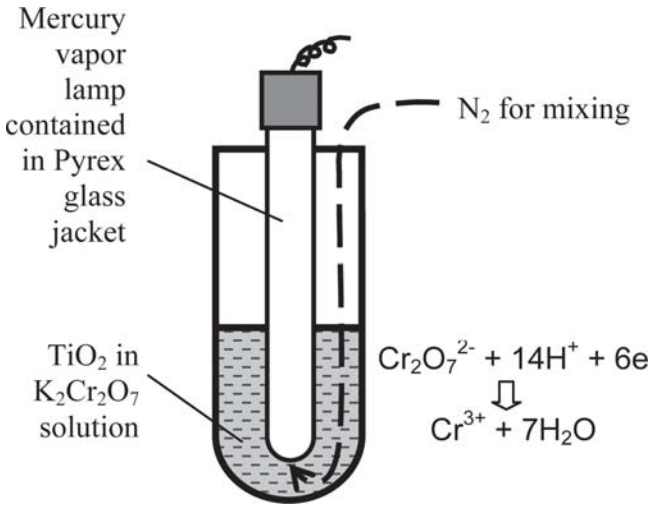

Fig. 3 Illustration of the device used to evaluate photocatalytic capacity of TiO_2. Chromate reduction reaction occurs by photocatalysis.

To evaluate the photocatalytic capacity, a straightforward device is used, as illustrated in Fig. 3.

For each analysis, 500 mg of ground TiO_2 powder is suspended in 500 mL of 150 μm $K_2Cr_2O_7$ solution contained in a quartz immersion well from Ace Glass (Vineland, NJ). A Philips H33CD 400 watt mercury vapor lamp wrapped in a Pyrex glass jacket is then immersed in the titania suspension. Nitrogen gas and a magnetic stirrer are used to mix the reagents. The clock is started immediately after the nitrogen begins to flow, but during the first 40 min of vigorous mixing, the mercury lamp is left off. This is purposely done to reduce the possibility of false readings caused by adsorption of dichromate ions by TiO_2 powders. The adsorption can cause decreases in $Cr_2O_7^{2-}$ concentration, which gives the perception that the photocatalyst is working. After this 30 min "black-out" period, it is reasonable to assume that the adsorption has reached its saturation point and will not affect the outcome. At this point, 10 mL of the mixture is removed from the reactor by a syringe to be used as the time = 0 background. The TiO_2 powders are removed with XPERTEK PTFE (Cobert Associates Inc., St. Louis, MO) syringe filters (pore size: 200 nm). The lamp is then ignited to start the illumination process. Every 20 min, a sample of the mixture (10 mL) is removed and filtered for subsequent analysis. During the entire illumination process, the device is tightly covered with aluminum foil to provide the maximum output from the lamp and also to prevent environmental stray light from affecting the results.

The absorption of these samples solutions was then measured spectrophotometrically at 350 nm, the absorption maximum of the dichromate solution. Several absorption readings are averaged and then converted into concentrations of dichromate anions via use of a Beer's law calibration curve. The data are then plotted against time, which shows how much dichromate anions have been reduced with the increase of time.

3. Results and Discussion

3.1 Plasma Treatment

After the plasma treatment in aqueous media, the color of rutile powders turned from pure white to purple. The color became darker with longer treatment time. When rutile was

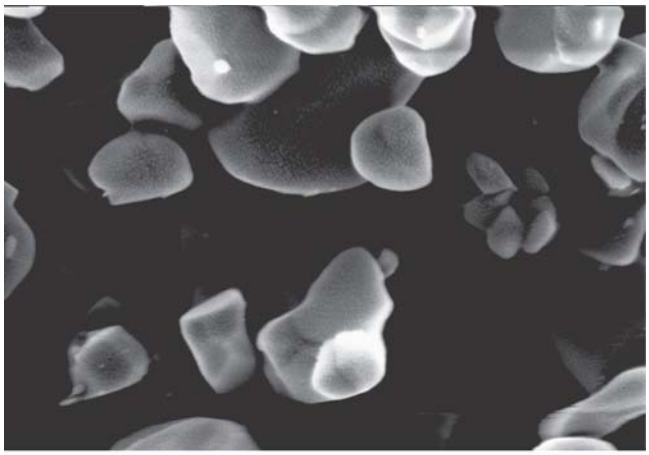

(a)

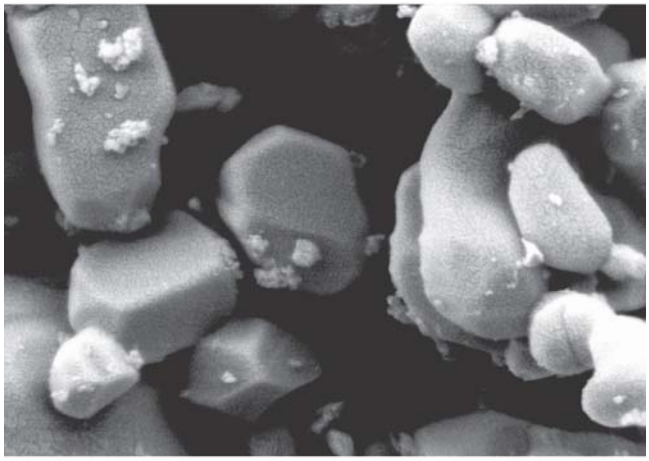

(b)

Fig. 4 SEM images of (a) unmodified rutile and (b) Fe/C-doped rutile (original magnification 50,000×)

suspended in acetonitrile, the color of the rutile turned from white to dark gray. This color change results from deposition of carbon nanoparticles on the rutile powder. These color variations suggest that, instead of absorbing almost nothing in the visible range, the rutile TiO_2 powders were red-shifted to absorb some visible light. However, it is not clear at this time whether the visible absorption is sufficiently strong to create electron/hole pairs to participate in the photocatalytic reactions.

Figure 4 shows the SEM images of the unmodified rutile and the Fe/C-doped rutile. Because plasma modification is extremely surface-oriented, it is understandable that the images show almost no changes in morphology. However, in the image of Fe/C-doped rutile (i.e., TiO_2 suspended in acetonitrile and treated with iron electrodes), small particles can be seen on the surface of the rutile particles. These are carbon nanoparticles that are products of dehydrogenation and fragmentation of acetonitrile molecules. Detailed information about the synthesis of carbon nanoparticles by DMP technology has been presented earlier (Ref 20, 21).

ICP-MS analysis was used to measure the concentration of Fe in plasma-treated rutile samples. It ranges from 2.0 to 4.0 mg/g (i.e., 0.2-0.4%). Because it is known that the solubility limit of iron in anatase TiO_2 is about 1% (Ref 22), the extent of iron doping can be considered to be fairly high in this DMP plasma treatment.

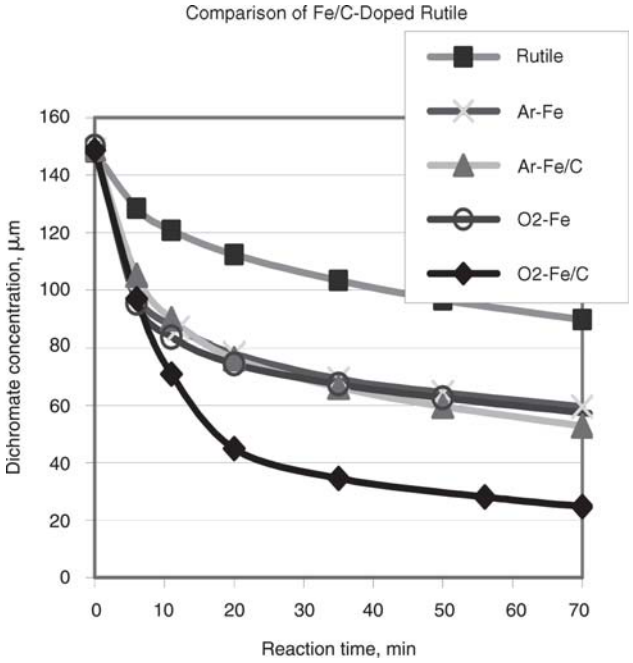

Fig. 5 Photoreactivity of plasma-treated rutile using different plasma gases

3.2 Photocatalytic Evaluation

To obtain the relationship between absorption and concentration, a set of solutions with known concentrations were measured. The data were then used to determine the two constants in Beer's law, and hence the following equation was obtained:

$$\text{Absorption} = 3.12717 \times \text{Concentration} + 0.00423$$

With this relationship, the concentrations of dichromate ions were calculated for all of the sample solutions taken from the quartz immersion well during illumination. The Cr concentrations are plotted against illumination/reaction time for evaluation of photocatalytic activity.

3.3 Impact of Different Plasma Gases

The first set of data, Fig. 5, shows the impact on photoreactivity caused by different plasma gases. For the purpose of comparison, two types of doping were used during the treatment: Fe or Fe/C (the carbon comes from the acetonitrile-originated nanoparticles). According to the figure, the following major conclusions can be made:

- O_2-treated, Fe/C-doped rutile exhibits the largest improvement in photoreactivity when compared with that of untreated rutile.
- Under the same condition, i.e., with the same doping, O_2 plasma tends to outperform Ar. This suggests that metal oxide (e.g., Fe_2O_3) plays a more important role in the photocatalytic improvement. This is understandable, given the fact that Fe has a band gap of only 2.2 eV and the excitation of 3*d* electrons of Fe^{3+} can contribute to the conduction band of TiO_2.
- Carbon might be involved in the interfacial charge transfer

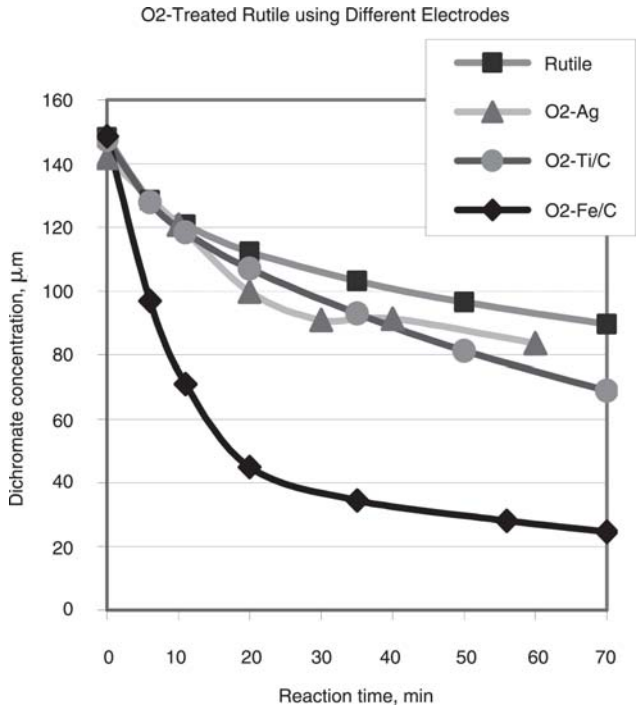

Fig. 6 Photoreactivity of oxygen-plasma-treated rutile with different doping elements

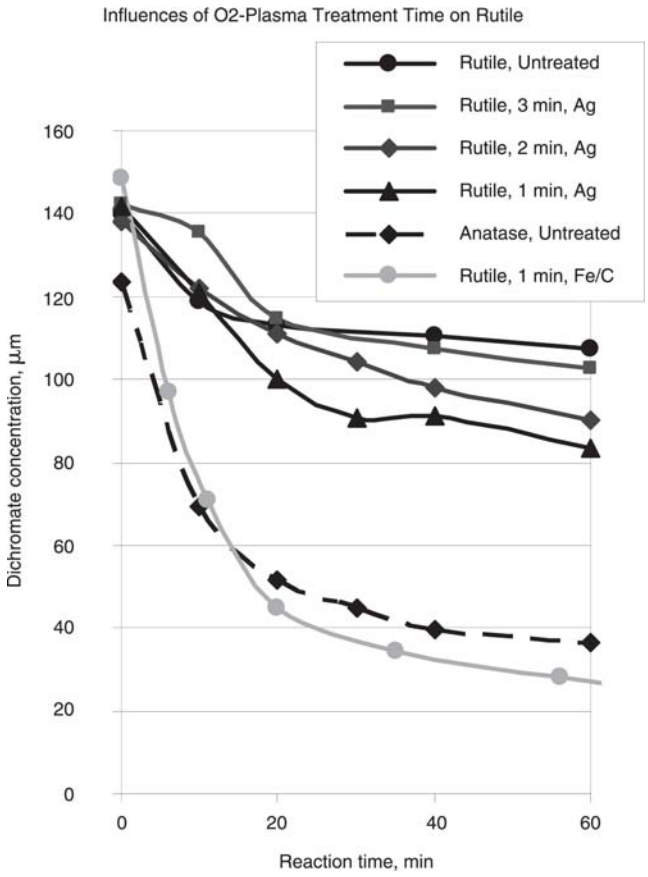

Fig. 7 Photoreactivity of oxygen-plasma-treated rutile with different treatment time. Untreated P25 anatase is also shown here for comparison.

reactions that are responsible for the improved photoreactivity. It may help accelerate the absorption of surrounding reaction molecules onto the TiO_2 surfaces or serve as electron traps to decrease the recombination possibility of electron/hole pairs.

3.4 Impact of Different Electrodes

By varying the electrode materials, the metal doping elements can be changed. The data in Fig. 6 show the influences of different doping metals on photoreactivity. Because previously mentioned results show that O_2 tends to perform better than Ar under the same conditions, oxygen was selected in this set of experiment.

From Fig. 6, it is very clear that, although silver and titanium improve the photoreactivity of rutile to some extent, it is the combination of iron and carbon nanoparticles that has the most dramatic effect. This result is in accord with the conclusion made in the previous subsection, i.e., that O_2-treated and Fe/C-doped rutiles show the biggest improvement.

3.5 Impact of Different Treatment Time

Finally, the influence of plasma treatment time on photoreactivity was evaluated. Data are presented in Fig. 7. To compare them directly, the same silver electrode and oxygen gas were used for all three plasma treatments, i.e., 1, 2, and 3 min.

The results show that longer treatment time, which should supposedly lead to higher Ag concentration, actually decreases the photoreactivity of rutile. This might be explained by a process similar to catalyst poisoning: a higher concentration of the doping elements reduces available reactive sites in contact with the surrounding reaction media and thus decreases the photocatalytic efficiency.

In addition to the data resulting from different treatment times, another set of curves is presented in Fig. 7, i.e., the photoreactivity of untreated P25 anatase and the best-performing plasma-treated rutile (O_2-treated, Fe/C-doped, and 1 min treatment time). It is noteworthy that the Fe/C-doped rutile shows much improved photocatalytic capacity and is, in fact, comparable to or even better than that of untreated anatase. This represents a very significant improvement in rutile photocatalytic activity.

In light of the above results, it is obvious that the DMP-induced doping of iron and the incorporation of carbon nanoparticles substantially improved the photoreactivity of rutile TiO_2. This improvement might be explained by one or more of the following mechanisms: the metal elements may have acted as electron traps, enhanced the electron/hole separation process, and thus extended the life time of the oxidizing power of the photocatalyst; the dipole moment from plasmon resonance effects in the metals may help the electron/hole separation; the various doping elements may have structurally modified the structure of the photocatalyst and thus increased its photoreactivity; carbon nanoparticles may have facilitated the transfer of surrounding reaction molecules, which lead to high efficiency of photoreactions.

At last, due to the limitations of our current analytical techniques, we still do not yet know whether the plasma modification performed on rutile has shifted its photoresponse wavelength toward the visible range, which would certainly result in much more efficient utilization of the solar energy. In our future work, the output spectrum of the light source will be

determined; if necessary, cutoff filters will be used to block the UV light, so that photoreactivity in the visible range can be evaluated.

4. Conclusions

Dense-medium plasma technology has been successfully used to modify rutile TiO_2. To determine the optimum parameters for the modification, three sets of treatment conditions were evaluated: different plasma gas, different doping materials, and different treatment times. It turns out that (a) oxygen plasma tends to be more efficient than Ar, indicating that metal oxides (e.g., Fe_2O_3) might play important roles; (b) among the four different types of doping elements used, the combination of iron and carbon nanoparticles results in dramatically improved photoreactivity; and (c) prolonged plasma treatment times actually decrease the photoreactivity of rutile due to mechanisms similar to that of catalyst poisoning.

Finally, it was found that the photoreactivity of O_2/1 min treated and Fe/C-doped rutile is comparable to or even better than that of untreated P25 anatase. Possible mechanisms for improvement were discussed.

Acknowledgment

The authors thank R. Rowell for his help with the ICP-MS analysis.

References

1. A. Fujishima and K. Honda, Electrochemical Photolysis of Water at a Semiconductor Electrode, *Nature,* 1972, **238,** p 37-38
2. A. Fujishima, K. Hashimoto, and T. Watanabe, *TiO_2 Photocatalysis: Fundamentals and Applications,* BKC, Inc., Tokyo, 1999
3. S. Yin, Q. Zhang, F. Saito, and T. Sato, Preparation of Visible Light-Activated Titania Photocatalyst by Mechanochemical Method, *Chem. Lett. (Jpn.),* 2003, **32**(4), p 358-359
4. L. Zhang, J.C. Yu, H.Y. Yip, Q. Li, K.W. Kwong, A.-W. Xu, and P.K. Wong, Ambient Light Reduction Strategy to Synthesize Silver Nanoparticles and Silver-Coated TiO_2 with Enhanced Photocatalytic and Bactericidal Activities, *Langmuir,* 2003, **19,** p 10372-10380
5. A. Orlov, D.A. Jefferson, N. Macleod, and R.M. Lambert, Photocatalytic Properties of TiO_2 Modified with Gold Nanoparticles in the Degradation of 4-Chlorophenol in Aqueous Solution, *Catal. Lett.,* 2004, **92**(1-2), p 41-47
6. V. Subramanian, E. Wolf, and P.V. Kamat, Semiconductor-Metal Composite Nanostructures. To What Extent Do Metal Nanoparticles Improve the Photocatalytic Activity of TiO_2 Films, *J. Phys. Chem. B,* 2001, **105**(46), p 11439-11446
7. N.R. de Tacconi, J. Carmona, and K. Rajeshwar, Chemically Modified Ni/TiO_2 Nanocomposite Films: Charge Transfer from Photoexcited TiO_2 Particles to Hexacyanoferrate Redox Centers within the Film and Unusual Photoelectrochemical Behavior, *J. Phys. Chem. B,* 1997, **101**(49), p 10151-10154
8. C. Wang, D.W. Bahnemann, J.K. Dohrmann, A Novel Preparation of Iron-Doped TiO_2 Nanoparticles with Enhanced Photocatalytic Activity, *Chem. Commun.*, 2000, p 1539
9. E. Stathatos, T. Petrova, and P. Lianos, Study of the Efficiency of Visible-Light Photocatalytic Degradation of Basic Blue Adsorbed on Pure and Doped Mesoporous Titania Films, *Langmuir,* 2001, **17**(16), p 5025-5030
10. R. Asahi, T. Morikawa, T. Ohwaki, K. Aoki, and Y. Taga, Visible-Light Photocatalysis in Nitrogen-Doped Titanium Oxides, *Science,* 2001, **293**(5528), p 269-271
11. T. Umebayashi, T. Yamaki, S. Tanaka, and K. Asai, Visible Light-Induced Degradation of Methylene Blue on S-Doped TiO_2, *Chem. Lett. (Jpn.),* 2003, **32**(4), p 330-331
12. S.U.M. Khan, M. Al-Shahry, and W.B. Ingler, Jr., Efficient Photochemical Water Splitting by a Chemically Modified n-TiO_2, *Science,* 2002, **297**(5590), p 2243-2245
13. S. Sakthivel and H. Kisch, Daylight Photocatalysis by Carbon-Modified Titanium Dioxide, *Angew. Chem. Int. Ed.,* 2003, **42**(40), p 4908-4911
14. H. Irie, Y. Watanabe, and K. Hashimoto, Carbon-Doped Anatase TiO_2 Powders as a Visible-Light Sensitive Photocatalyst, *Chem. Lett. (Jpn.),* 2003, **32**(8), p 772-773
15. Y. Choi, S. Yamamoto, H. Saitoh, T. Sumita, and H. Itoh, Influence of Carbon-Ion Irradiation and Hydrogen-Plasma Treatment on Photocatalytic Properties of Titanium Dioxide Films, *Phys. Res. B,* 2003, **206,** p 241-244
16. P.A.M. Hotsenpiller, J.D. Bolt, W.E. Farneth, J.B. Lowekamp, and G.S. Rohrer, Orientation Dependence of Photochemical Reactions on TiO_2 Surfaces, *J. Phys. Chem. B,* 1998, **102**(17), p 3216-3226
17. R.I. Bickley, T. Gonzalez-Carreno, J.S. Lees, L. Palmisano, and R.J.D. Tilley, A Structural Investigation of Titanium Dioxide Photocatalysts, *J. Solid State Chem.,* 1991, **92**(1), p 178-190
18. F.S. Denes and R.A. Young, Apparatus for Reaction in Dense Medium Plasmas, U.S. Patent 5 534 232
19. F.S. Denes, R.A. Young, and Z.Q. Hua, Methods for Reactions in Dense-Medium Plasmas and Products Formed Thereby, U.S. Patent 5 908 539
20. F. Denes, S. Manolache, Y.C. Ma, V. Shamamian, B. Ravel, and S. Prokes, Dense Medium Plasma Synthesis of Carbon/Iron-Based Magnetic Nanoparticle System, *J. Appl. Phys.,* 2003, **94**(5), p 3498-3508
21. Y. Ma, S. Manolache, F. Denes, D. Thamm, I. Kurzman, and D. Vail, Plasma Synthesis of Carbon Magnetic Nanoparticles and Immobilization of Doxorubicin for Targeted Drug Delivery, *J. Biomater. Sci. Polym. Ed.,* 2004, **15**(8), p 1033-1049
22. W. Zhang, Y. Li, S. Zhu, and F. Wang, Fe-Doped Photocatalytic TiO_2 Film Prepared by Pulsed DC Reactive Magnetron Sputtering, *J. Vac. Sci. Technol. A,* 2003, **21**(6), p 1877-1882